

Research Article

Improved Photocatalytic Performance of a Novel $\text{Fe}_3\text{O}_4@\text{SiO}_2/\text{Bi}_2\text{SiO}_5$ Hierarchical Nanostructure with Magnetic Recoverability

Xinxin Zhang, Xiaoli Dong, Baiyu Leng, Hongchao Ma, and Xiufang Zhang

School of Light Industry and Chemical Engineering, Dalian Polytechnic University, Dalian 116034, China

Correspondence should be addressed to Xiaoli Dong; dongxl@dlpu.edu.cn and Hongchao Ma; m-h-c@sohu.com

Received 6 August 2015; Accepted 25 October 2015

Academic Editor: Ahmad Umar

Copyright © 2015 Xinxin Zhang et al. This is an open access article distributed under the Creative Commons Attribution License, which permits unrestricted use, distribution, and reproduction in any medium, provided the original work is properly cited.

Magnetic $\text{Fe}_3\text{O}_4@\text{SiO}_2/\text{Bi}_2\text{SiO}_5$ composites with a novel hierarchical nanostructure were synthesized by sol-gel and hydrothermal methods and were characterized by scanning electron microscopy (SEM), X-ray diffraction (XRD), Fourier transform infrared spectroscopy (FTIR), X-ray photoelectron spectroscopy (XPS), and UV-visible diffuse reflectance spectroscopy (UV-vis DRS). It was found that the introduction of $\text{Fe}_3\text{O}_4@\text{SiO}_2$ could turn the morphology of Bi_2SiO_5 from close-grained slab to hollow hierarchical architecture with fabric-structure. The $\text{Fe}_3\text{O}_4@\text{SiO}_2/\text{Bi}_2\text{SiO}_5$ composite showed enhanced photodegradation efficiency for the degradation of reactive brilliant red dye (X-3B) in aqueous solution under simulated sunlight irradiation, as compared with that of commercial P25. In addition, the $\text{Fe}_3\text{O}_4@\text{SiO}_2/\text{Bi}_2\text{SiO}_5$ composite exhibited good magnetic recoverability and excellent photocatalytic stability (no obvious activity loss after recycling tests).

1. Introduction

Photocatalysis has been extensively used for degradation of numerous organic pollutants [1, 2]. In photocatalytic process, the photocatalytic materials play a crucial role in realizing its practical applications. Recently, bismuth-based photocatalysts have been widely reported owing to their excellent photocatalytic performance, such as Bi_2GeO_5 [3], Bi_2MoO_6 [4, 5], Bi_2WO_6 [6], and Bi_2SiO_5 [7]. Bi_2SiO_5 , one of the family, consists of an interaction of two $(\text{Bi}_2\text{O}_2)^{2+}$ layers and $(\text{SiO}_3)^{2-}$ pyroxene layers inserted between $(\text{Bi}_2\text{O}_2)^{2+}$ layers. The $(\text{Bi}_2\text{O}_2)^{2+}$ layers are made up of slightly distorted squared oxygen planes. These squares are capped alternatively above and below by the bismuth atoms. The distorted feature of SiO_4 tetrahedra could be a benefit for splitting photogenerated electrons and holes. Thus, good photocatalytic activity of the Bi_2SiO_5 should be expected [8, 9].

Nevertheless, photocatalysts are normally used as suspension in the photocatalytic process. Some processes for separation of suspended catalyst are necessary, such as centrifugation and filtration. And, some loss of catalyst during these separation processes is the major drawback.

To overcome this problem, immobilization of photocatalysts on various easily recoverable materials including glass beads [10], glass fibers [11], and ceramic plates [12] has been studied. However, these methods resulted in significant decrease of photocatalytic efficiency because of the decreased surface area of catalyst coated on the support. Thus, the effective removal of nanosized catalyst powders from the treated water suspension is a challenge for recovery of catalyst.

It is well known that magnetic materials could be easily recovered by applying a magnetic field [13, 14]. Thus, if the photocatalyst contains a magnetic material, recovery of the photocatalyst from an aqueous system by applying external magnetic field is attractive for commercial application. In general, the magnetic photocatalysts were composed mainly of catalyst coating, inertial layer (SiO_2 or Al_2O_3), and the magnetic core material (Fe_3O_4) [15, 16]. The inertial layer (SiO_2 or Al_2O_3) plays a key role to avoid photodissolution phenomenon of magnetic core material, which is an electronic interaction between catalyst coating and the magnetic core.

Herein, magnetic $\text{Fe}_3\text{O}_4@\text{SiO}_2/\text{Bi}_2\text{SiO}_5$ composites with hierarchical nanostructure were fabricated for the

improvement of the photocatalytic performance and easy separation. X-3B, a common pollutant in the industry wastewater, was selected as a test substance to evaluate the photocatalytic performance of prepared photocatalysts. Noteworthy, the as-prepared composites not only exhibited excellent photocatalytic activity for the degradation of X-3B but also are easily recycled via an external magnetic field.

2. Experimental Section

2.1. Reagents and Materials. The $\text{Bi}(\text{NO}_3)_3 \cdot 5\text{H}_2\text{O}$, $\text{FeCl}_3 \cdot 6\text{H}_2\text{O}$, ethylene glycol, $\text{NH}_3 \cdot \text{H}_2\text{O}$, tetraethyl orthosilicate (TEOS), reactive brilliant Red X-3B dye (X-3B), and $\text{Na}_2\text{SiO}_3 \cdot 9\text{H}_2\text{O}$ were purchased from Tianjin Chemical Reagents Company. All these reagents were of AR grades and were used without further purification.

2.2. Preparation of Samples

2.2.1. Preparation of Fe_3O_4 . The typical synthesis procedure is as follows: 0.1 M $\text{FeCl}_3 \cdot 6\text{H}_2\text{O}$, 0.8 M sodium acetate, and 0.09 M sodium citrate were dispersed in 60 mL ethylene glycol with magnetic stirrer for 1 h at room temperature. The as-obtained mixture was transferred into a Teflon-lined stainless-steel autoclave with a capacity of 100 mL and then heated at 200°C for 12 h. The final product was collected with a magnet and washed with deionized water and anhydrous ethanol for several times and then dried at 60°C for 3 h in air.

2.2.2. Preparation of $\text{Fe}_3\text{O}_4 @ \text{SiO}_2$. Firstly, 0.75 g Fe_3O_4 MNPs was redispersed into 170 mL ethanol. The mixture was homogenized by ultrasonication for 20 min after adding 1 mL ammonium hydroxide ($\text{NH}_3 \cdot \text{H}_2\text{O}$). After that, as-obtained mixture was vigorously stirred with a mechanical agitator at 30°C for 30 min; then, 1.0 mL tetraethyl orthosilicate (TEOS) was introduced dropwise into the solution. The final product was separated by external magnetic field.

2.2.3. Preparation of $\text{Fe}_3\text{O}_4 @ \text{SiO}_2 / \text{Bi}_2\text{SiO}_5$. In a typical process [7], a desired amount of $\text{Fe}_3\text{O}_4 @ \text{SiO}_2$ MNPs (0, 0.05, 0.1, 0.2, and 0.3 g) was dispersed in 75 mL deionized water under ultrasonication for 20 min. Then, 0.05 M $\text{Bi}(\text{NO}_3)_3 \cdot 5\text{H}_2\text{O}$ and 0.025 M $\text{Na}_2\text{SiO}_3 \cdot 9\text{H}_2\text{O}$ were added into the above suspension. The pH value of solution was adjusted to 9 by adding $\text{NH}_3 \cdot \text{H}_2\text{O}$. After ultrasonication for 30 min, the mixture was transferred into a Teflon-lined stainless-steel autoclave and then heated at 180°C for 48 h. Finally, the autoclave was cooled down to room temperature naturally. The products were collected and washed with deionized water and anhydrous ethanol several times and then dried at 80°C for 6 h. The sample is labeled as BSO-0, BSO-0.05, BSO-0.1, BSO-0.2, and BSO-0.3. Furthermore, pure Bi_2SiO_5 for reference was also prepared using the same method without $\text{Fe}_3\text{O}_4 @ \text{SiO}_2$ nanoparticle.

2.3. Characterizations. The morphology of the samples was displayed using scanning electron microscopy (SEM) on a JSM 6460LV instrument (JEOL Ltd.) operated at 20 kV and

equipped with an energy-dispersive X-ray analyzer (Phoenix Ltd.). The X-ray diffraction (XRD) analysis of as-obtained samples was performed on a Shimadzu XRD-6100 diffractometer (Shimadzu Ltd.) at 40 kV and 40 mA with Cu K α radiation. Fourier transform infrared spectroscopy (FTIR) of product was recorded on a Shimadzu IRAffinity-1 (Shimadzu Ltd.) with a resolution of 4 cm^{-1} . X-ray photoelectron spectroscopy (XPS) measurement was done with a VGESCALAB 250 spectrometer (ThermoFisher Scientific) equipped with a monochromated Al-K α radiation source (1486.6 eV). UV-vis diffuse reflectance spectra were recorded on a CARY-100 spectrometer (VARIAN Ltd.) and BaSO_4 was used as a reflectance standard.

2.4. Photocatalytic Activity Measurements. The photocatalytic activity of the prepared catalysts was estimated by measuring the degradation rate of X-3B (40 mg/L) in an aqueous solution under sunlight. 0.1 g of photocatalyst was added in quartz reactor containing 100 mL dye aqueous solution with air stirring. The 400 W xenon lamp was used to get simulated sunlight. In the process of degradation, a certain volume of suspension was sampled under interval of 20 min and then centrifuged immediately to remove the particles. The absorbance of solution was measured by a UV-1800PC spectrophotometer (MAPADA, China) at 538 nm, and the degradation rate (R_x) of X-3B was calculated by the following expression:

$$R_x = \frac{(A_0 - A_t)}{A_0} \times 100\%, \quad (1)$$

in which A_0 was the absorbance of initial solution of X-3B and A_t was the absorbance of the solution of X-3B.

3. Results and Discussion

The SEM images of $\text{Fe}_3\text{O}_4 @ \text{SiO}_2$ and $\text{Fe}_3\text{O}_4 @ \text{SiO}_2 / \text{Bi}_2\text{SiO}_5$ composites are shown in Figure 1. As shown in Figure 1(a), the $\text{Fe}_3\text{O}_4 @ \text{SiO}_2$ particles are spherical with uniform size, and the average particle size is about 500 nm. From Figure 1(b), it can be seen that pure Bi_2SiO_5 sample exhibits close-grained slab microstructure. Nevertheless, introducing $\text{Fe}_3\text{O}_4 @ \text{SiO}_2$ changed obviously the morphology and microstructure of Bi_2SiO_5 (seeing Figures 1(c)–1(f)). The introduction of $\text{Fe}_3\text{O}_4 @ \text{SiO}_2$ turned the morphology of Bi_2SiO_5 from close-grained slab to hollow hierarchical architecture with fabric structure. Further SEM observation reveals that the hollow hierarchical architecture is constructed by exclusive knitting of a large quantity of irregular nanosheets. In addition, it is also clearly observed that more and more spherical $\text{Fe}_3\text{O}_4 @ \text{SiO}_2$ nanoparticles are embedded on the surface of hollow hierarchical Bi_2SiO_5 architecture with increase of $\text{Fe}_3\text{O}_4 @ \text{SiO}_2$ loadings. The hierarchical Bi_2SiO_5 architectures possess many open pores derived from the self-arrangement of nanosheets, which could promote multiple scattering of the incident light and lead to an enhanced light-harvesting capacity. It is believed that the hollow hierarchical microstructures are ideal materials for potential applications in photocatalytic process.

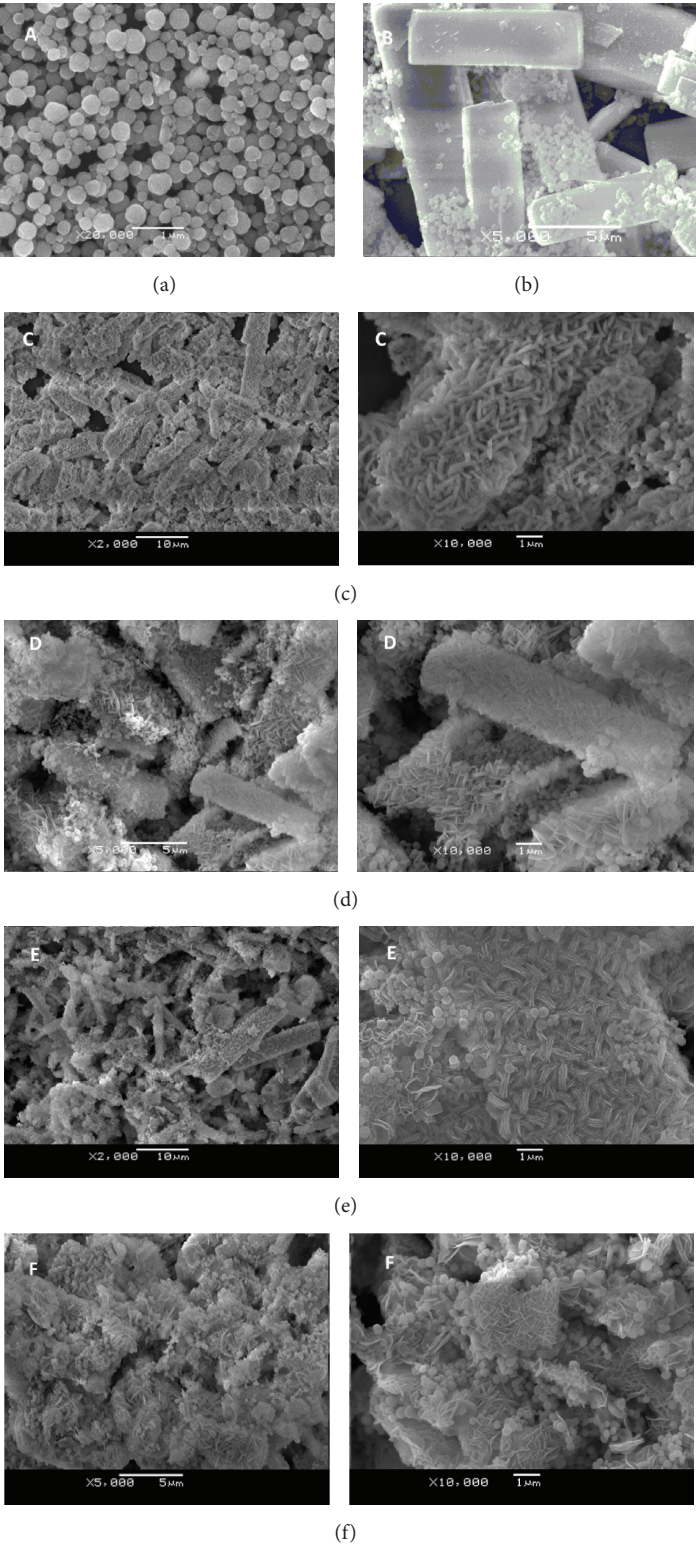


FIGURE 1: SEM images of samples ((a) $Fe_3O_4@SiO_2$, (b) BSO-0, (c) BSO-0.05, (d) BSO-0.1, (e) BSO-0.2, and (f) BSO-0.3).

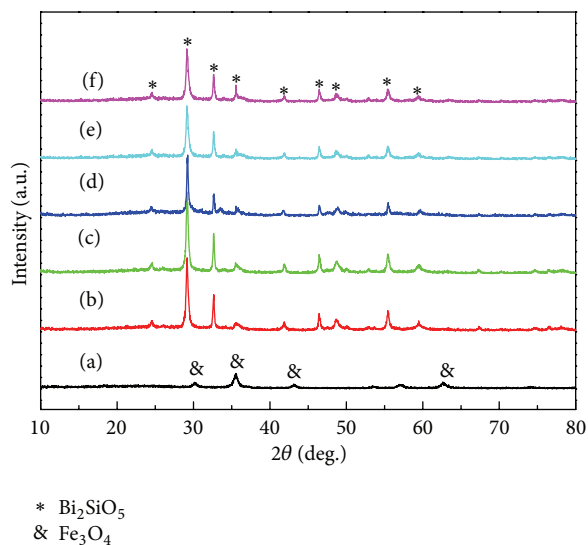


FIGURE 2: XRD patterns of samples ((a) $\text{Fe}_3\text{O}_4@SiO_2$, (b) BSO-0, (c) BSO-0.05, (d) BSO-0.1, (e) BSO-0.2, and (f) BSO-0.3).

Phase structures of the as-prepared samples were examined by powder XRD analysis and are shown in Figure 2. For Figure 1(a), all diffraction peaks can be indexed to the Fe_3O_4 phase (JCPDS number 15-7609). Figure 2(b–f) depicts XRD patterns of $\text{Fe}_3\text{O}_4@SiO_2/Bi_2SiO_5$ composites with different quantities of $\text{Fe}_3\text{O}_4@SiO_2$. As shown in Figure 2(b–f), all the diffraction peaks could be perfectly indexed to the tetragonal phase of Bi_2SiO_5 (JCPDS 36-0288). No diffraction peak of Fe_3O_4 was detected, which may be attributed to incorporation of the magnetic cores in Bi_2SiO_5 microstructures.

The composition and structure of the products were also measured by infrared (IR) spectra. As shown in Figure 3, the typical Fe-O stretching bands at 584 cm^{-1} can be found in all samples, indicating existence of magnetic core in composites. The $\text{Fe}_3\text{O}_4@SiO_2$ sample showed the bending, symmetric and asymmetric stretching vibration of Si-O-Si at 482 cm^{-1} , 790 cm^{-1} , and 1083 cm^{-1} , respectively. Furthermore, the bands attributed to vibration of Si-O around 1224 cm^{-1} [17] can also be observed in $\text{Fe}_3\text{O}_4@SiO_2$ sample. This result indicates that Fe_3O_4 microspheres were wrapped by SiO_2 . Moreover, the characteristic bands of Bi_2SiO_5 can be observed from IR spectrum of $\text{Fe}_3\text{O}_4@SiO_2/Bi_2SiO_5$ composite, such as the Bi-O-Si vibration at 894 cm^{-1} and 1020 cm^{-1} originated from $(SiO_5)^{6-}$. Nevertheless, $\text{Fe}_3\text{O}_4@SiO_2/Bi_2SiO_5$ composite still possesses abundant surface O-H bond located at 1637 cm^{-1} , which could enhance the photocatalytic activity owing to the -OH offering larger capacity for oxygen adsorption [18].

The optical properties of $\text{Fe}_3\text{O}_4@SiO_2/Bi_2SiO_5$ hierarchical nanostructure were also investigated by UV-vis DRS. As a comparison, the spectra of Bi_2SiO_5 and TiO_2 were also measured. As shown in Figure 4, the intense absorption of Bi_2SiO_5 in the UV light regions was similar to that of TiO_2 , which indicated that the Bi_2SiO_5 could be used as an effective photocatalyst to degrade various pollutants [7, 19]. It is worth noting that $\text{Fe}_3\text{O}_4@SiO_2/Bi_2SiO_5$ composites showed the

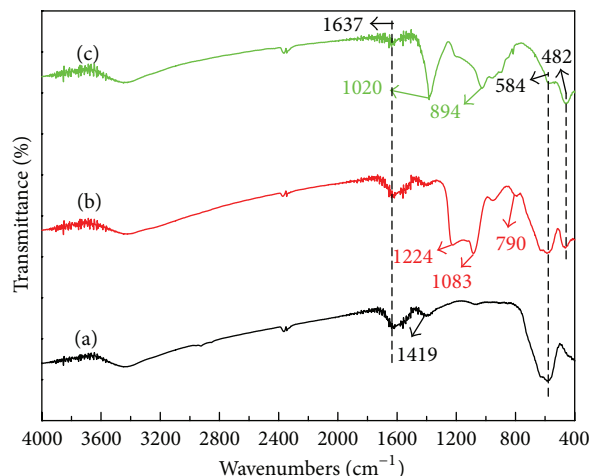


FIGURE 3: IR spectra of (a) Fe_3O_4 , (b) $\text{Fe}_3\text{O}_4@SiO_2$, and (c) $\text{Fe}_3\text{O}_4@SiO_2/Bi_2SiO_5$.

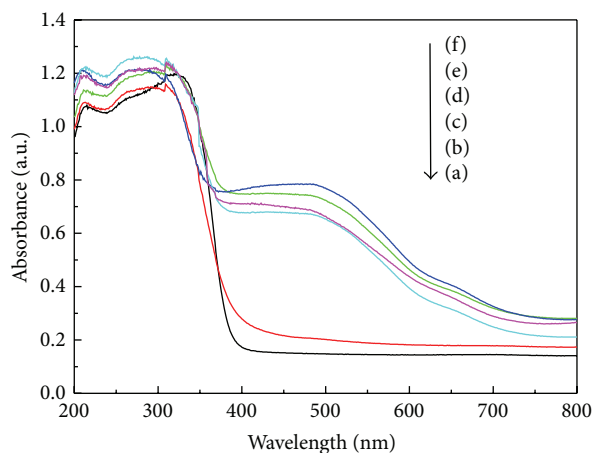


FIGURE 4: UV-vis absorption spectra of samples ((a) P25, (b) BSO-0, (c) BSO-0.05, (d) BSO-0.1, (e) BSO-0.2, and (f) BSO-0.3).

stronger absorption in visible light region, as compared with that of sample Bi_2SiO_5 . With the increase of the mass fraction of $\text{Fe}_3\text{O}_4@SiO_2$, the absorption intensity of visible light region becomes stronger, which can be attributed to introducing of magnetic cores. Obviously, the strong absorption in visible light region is favorable to enhance utilization efficiency of sunlight.

3.1. Photocatalytic Activity Analysis. The photocatalytic performance of the as-prepared samples was measured under irradiation of simulated solar light. It can be seen from Figure 5 that Bi_2SiO_5 and $\text{Fe}_3\text{O}_4@SiO_2/Bi_2SiO_5$ composites exhibit the better photocatalytic activity under irradiation of simulated solar light, as compared with P25. Nevertheless, the activity of as-prepared $\text{Fe}_3\text{O}_4@SiO_2/Bi_2SiO_5$ composites did not monotonously increase with increase of $\text{Fe}_3\text{O}_4@SiO_2$ content. The BSO-0.2 sample showed best photocatalytic activity, and the photodegradation rate can reach 65% after irradiation for 120 min. The highly enhanced photocatalytic

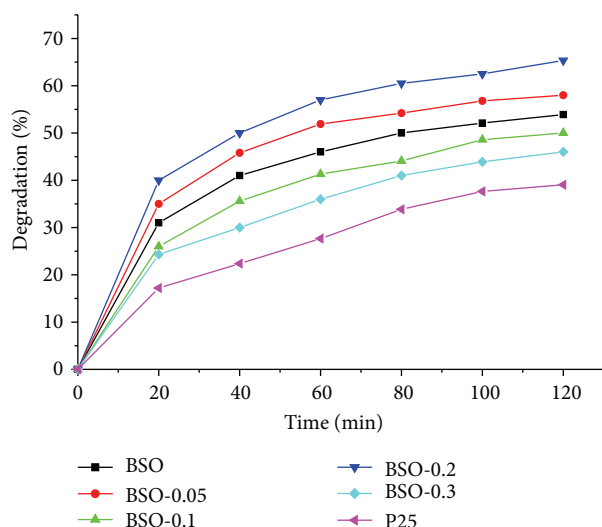


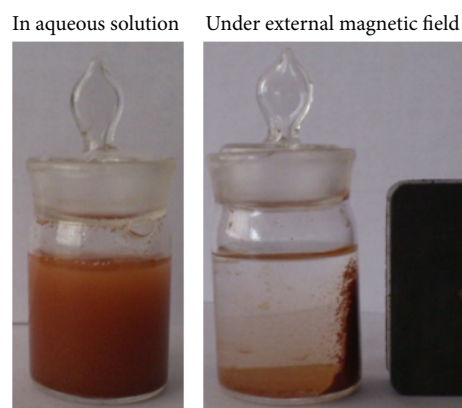
FIGURE 5: Photocatalytic performance of $\text{Fe}_3\text{O}_4@/\text{SiO}_2/\text{Bi}_2\text{SiO}_5$ composites and P25.

activity of $\text{Fe}_3\text{O}_4@/\text{SiO}_2/\text{Bi}_2\text{SiO}_5$ composites under simulated solar light irradiation can be attributed to (1) the introduction of $\text{Fe}_3\text{O}_4@/\text{SiO}_2$ which widened the range of spectral response and (2) the hollow hierarchical structure which could promote multiple scattering of the incident light and lead to an enhanced light-harvesting capacity.

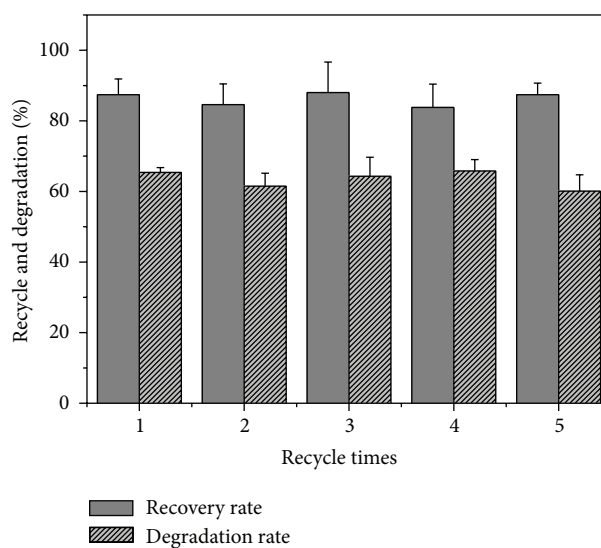
The stability and magnetic recoverability of $\text{Fe}_3\text{O}_4@/\text{SiO}_2/\text{Bi}_2\text{SiO}_5$ composite were also investigated. The magnetic recovering test was performed as illustrated in Figure 6. As shown in Figure 6(a), the $\text{Fe}_3\text{O}_4@/\text{SiO}_2/\text{Bi}_2\text{SiO}_5$ composite dispersed in an aqueous solution was easily recovered by external magnetic field. This result indicated that $\text{Fe}_3\text{O}_4@/\text{SiO}_2/\text{Bi}_2\text{SiO}_5$ composites are magnetically recoverable. Furthermore, the recycled photodegradation experiments were performed using BSO-0.2 owing to its high activity. The sample was recollectd by external magnetic field after each cycle. It can be seen from Figure 6(b) that the photocatalytic activity of photocatalyst did not exhibit an obvious loss of activity after five rounds. The results indicated that $\text{Fe}_3\text{O}_4@/\text{SiO}_2/\text{Bi}_2\text{SiO}_5$ composite possessed good durability during photocatalytic process.

4. Conclusions

In summary, the hollow hierarchical $\text{Fe}_3\text{O}_4@/\text{SiO}_2/\text{Bi}_2\text{SiO}_5$ composites with magnetic recoverability have been successfully prepared through simple hydrothermal method. $\text{Fe}_3\text{O}_4@/\text{SiO}_2/\text{Bi}_2\text{SiO}_5$ composites show highly photocatalytic activity under simulated solar light irradiation, as compared with that of pure Bi_2SiO_5 and P25. The highly photocatalytic performance of the $\text{Fe}_3\text{O}_4@/\text{SiO}_2/\text{Bi}_2\text{SiO}_5$ can be ascribed to the strong light absorption and high light-harvesting efficiency of hollow hierarchical structure. Furthermore, the synthesized magnetic composites can be recovered by external magnetic field, which can enhance the separation efficiency of photocatalyst in wastewater treatment.



(a)



(b)

FIGURE 6: (a) The recoverability of $\text{Fe}_3\text{O}_4@/\text{SiO}_2/\text{Bi}_2\text{SiO}_5$ composite under external magnetic field (b) the stability and recoverability of $\text{Fe}_3\text{O}_4@/\text{SiO}_2/\text{Bi}_2\text{SiO}_5$ composite.

Conflict of Interests

The authors declare that there is no conflict of interests regarding the publication of this paper.

Acknowledgments

The research was supported by the National Natural Science Foundation of China (Grant no. 21476033) and the Cultivation Program for Excellent Talents of Science and Technology Department of Liaoning Province (no. 201402610).

References

- [1] Y. Wang, S. K. Li, X. R. Xing et al., "Self-assembled 3D flowerlike hierarchical $\text{Fe}_3\text{O}_4@/\text{Bi}_2\text{O}_3$ core-shell architectures and their enhanced photocatalytic activity under visible light," *Chemistry—A European Journal*, vol. 17, no. 17, pp. 4802–4808, 2011.

- [2] X.-L. Dong, X.-Y. Mou, H.-C. Ma et al., "Preparation of CdS-TiO₂/Fe₃O₄ photocatalyst and its photocatalytic properties," *Journal of Sol-Gel Science and Technology*, vol. 66, no. 2, pp. 231–237, 2013.
- [3] R. G. Chen, J. H. Bi, L. Wu, Z. H. Li, and X. Z. Fu, "Orthorhombic Bi₂GeO₅ nanobelts: synthesis, characterization, and photocatalytic properties," *Crystal Growth & Design*, vol. 9, no. 4, pp. 1775–1779, 2009.
- [4] J. H. Bi, L. Wu, J. Li, Z. H. Li, X. X. Wang, and X. Z. Fu, "Simple solvothermal routes to synthesize nanocrystalline Bi₂MoO₆ photocatalysts with different morphologies," *Acta Materialia*, vol. 55, no. 14, pp. 4699–4705, 2007.
- [5] X. Zhao, J. H. Qu, H. J. Liu, and C. Hu, "Photoelectrocatalytic degradation of triazine-containing azo dyes at γ -Bi₂MoO₆ film electrode under visible light irradiation ($\lambda > 420$ nm)," *Environmental Science & Technology*, vol. 41, no. 19, pp. 6802–6807, 2007.
- [6] Y. Y. Li, J. P. Liu, X. T. Huang, and G. Y. Li, "Hydrothermal synthesis of Bi₂WO₆ uniform hierarchical microspheres," *Crystal Growth & Design*, vol. 7, no. 7, pp. 1350–1355, 2007.
- [7] R. G. Chen, J. H. Bi, L. Wu, W. J. Wang, Z. H. Li, and X. Z. Fu, "Template-free hydrothermal synthesis and photocatalytic performances of novel Bi₂SiO₅ nanosheets," *Inorganic Chemistry*, vol. 48, no. 19, pp. 9072–9076, 2009.
- [8] S. Geoges, F. Goutenoire, and P. Lacorre, "Crystal structure of lanthanum bismuth silicate Bi_{2-x}La_xSiO₅ (x~0.1)," *Journal of Solid State Chemistry*, vol. 179, pp. 4020–4028, 2006.
- [9] Y. Hou, L. Wu, X. Wang, Z. Ding, Z. Li, and X. Fu, "Photocatalytic performance of α -, β -, and γ -Ga₂O₃ for the destruction of volatile aromatic pollutants in air," *Journal of Catalysis*, vol. 250, no. 1, pp. 12–18, 2007.
- [10] N. B. Jackson, C. M. Wang, Z. Luo et al., "Attachment of TiO₂ powders to hollow glass microbeads: activity of the TiO₂-coated beads in the photoassisted oxidation of ethanol to acetaldehyde," *Journal of the Electrochemical Society*, vol. 138, no. 12, pp. 3660–3664, 1991.
- [11] R. L. Pozzo, M. A. Baltanás, and A. E. Cassano, "Supported titanium oxide as photocatalyst in water decontamination: state of the art," *Catalysis Today*, vol. 39, no. 3, pp. 219–231, 1997.
- [12] M. Bideau, B. Claudel, C. Dubien, L. Faure, and H. Kazouan, "On the 'immobilization' of titanium dioxide in the photocatalytic oxidation of spent waters," *Journal of Photochemistry and Photobiology A: Chemistry*, vol. 91, no. 2, pp. 137–144, 1995.
- [13] T. F. Jiao, Y. Z. Liu, Y. T. Wu et al., "Facile and scalable preparation of graphene oxide-based magnetic hybrids for fast and highly efficient removal of organic dyes," *Scientific Reports*, vol. 5, Article ID 12451, 2015.
- [14] W. Wang, T. F. Jiao, Q. R. Zhang et al., "Hydrothermal synthesis of hierarchical core-shell manganese oxide nanocomposites as efficient dye adsorbents for wastewater treatment," *RSC Advance*, vol. 5, no. 69, pp. 56279–56285, 2015.
- [15] Q. Yuan, N. Li, W. C. Geng, Y. Chi, and X. T. Li, "Preparation of magnetically recoverable Fe₃O₄@SiO₂@meso-TiO₂ nanocomposites with enhanced photocatalytic ability," *Materials Research Bulletin*, vol. 47, no. 9, pp. 2396–2402, 2012.
- [16] J. Liu, Z. K. Sun, Y. H. Deng et al., "Highly water-dispersible biocompatible magnetite particles with low cytotoxicity stabilized by citrate groups," *Angewandte Chemie International Edition*, vol. 48, no. 32, pp. 5875–5879, 2009.
- [17] Q. Gao, F. H. Chen, J. L. Zhang et al., "The study of novel Fe₃O₄@ γ -Fe₂O₃ core/shell nanomaterials with improved properties," *Journal of Magnetism and Magnetic Materials*, vol. 321, no. 8, pp. 1052–1057, 2009.
- [18] Z. Liu, X. Quan, H. Fu, X. Li, and K. Yang, "Effect of embedded-silica on microstructure and photocatalytic activity of titania prepared by ultrasound-assisted hydrolysis," *Applied Catalysis B: Environmental*, vol. 52, no. 1, pp. 33–40, 2004.
- [19] D. J. Yang, H. W. Liu, Z. F. Zheng et al., "An efficient photocatalyst structure: TiO₂(B) nanofibers with a shell of anatase nanocrystals," *Journal of the American Chemical Society*, vol. 131, no. 49, pp. 17885–17893, 2009.



Hindawi

Submit your manuscripts at
<http://www.hindawi.com>

